THE UNIVERSITY of EDINBURGH

Edinburgh Research Explorer

Making and breaking bridges in a Pickering emulsion

Citation for published version:
French, D, Taylor, P, Fowler, J & Clegg, PS 2015, 'Making and breaking bridges in a Pickering emulsion', *Journal of Colloid and Interface Science*, vol. 441, pp. 30-38. https://doi.org/10.1016/j.jcis.2014.11.032

Digital Object Identifier (DOI):
10.1016/j.jcis.2014.11.032

Link:
Link to publication record in Edinburgh Research Explorer

Document Version:
Publisher's PDF, also known as Version of record

Published In:
Journal of Colloid and Interface Science

Publisher Rights Statement:
This is an open access article under the CC BY license (http://creativecommons.org/licenses/by/3.0/).

General rights
Copyright for the publications made accessible via the Edinburgh Research Explorer is retained by the author(s) and / or other copyright owners and it is a condition of accessing these publications that users recognise and abide by the legal requirements associated with these rights.

Take down policy
The University of Edinburgh has made every reasonable effort to ensure that Edinburgh Research Explorer content complies with UK legislation. If you believe that the public display of this file breaches copyright please contact openaccess@ed.ac.uk providing details, and we will remove access to the work immediately and investigate your claim.

Download date: 06. May. 2023

Journal of Colloid and Interface Science 441 (2015) 30–38

Contents lists available at ScienceDirect

Journal of Colloid and Interface Science

www.elsevier.com/locate/jcis

Making and breaking bridges in a Pickering emulsion

David J. French [a,*], Phil Taylor [b], Jeff Fowler [c], Paul S. Clegg [a]

[a] School of Physics & Astronomy, The University of Edinburgh, Peter Guthrie Tait Road, Edinburgh EH9 3FD, UK
[b] Formulation Technology Group, Syngenta Crop Sciences, Jealott's Hill International Research Centre, UK
[c] Syngenta Inc., 410 Swing Rd, P.O. Box 183000, Greensboro, NC 27419-8300, USA

ARTICLE INFO

Article history:
Received 27 August 2014
Accepted 11 November 2014
Available online 20 November 2014

Keywords:
Pickering emulsions
Particle-stabilized emulsions
Particle bridging
Droplet adhesion
Aggregating droplets
Aggregating emulsion
Shear history
Process conditions

ABSTRACT

Hypothesis: Particle bridges form in Pickering emulsions when the oil–water interfacial area generated by an applied shear is greater than that which can be stabilised by the available particles and the particles have a slight preference for the continuous phase. They can subsequently be broken by low shear or by modifying the particle wettability.
Experiments: We have developed a model oil-in-water system for studying particle bridging in Pickering emulsions stabilised by fluorescent Stöber silica. A mixture of dodecane and isopropyl myristate was used as the oil phase. We have used light scattering and microscopy to study the degree to which emulsions are bridged, and how this is affected by parameters including particle volume fraction, particle wettability and shear rate. We have looked for direct evidence of droplets sharing particles using freeze fracture scanning electron microscopy.
Findings: We have created strongly aggregating Pickering emulsions using our model system. This aggregating state can be accessed by varying several different parameters, including particle wettability and particle volume fraction. Particles with a slight preference for the continuous phase are required for bridging to occur, and the degree of bridging increases with increasing shear rate but decreases with increasing particle volume fraction. Particle bridges can subsequently be removed by applying low shear or by modifying the particle wettability.
© 2014 The Authors. Published by Elsevier Inc. This is an open access article under the CC BY license (http://creativecommons.org/licenses/by/3.0/).

1. Introduction

Particle-stabilised, or Pickering, emulsions have received a lot of attention in recent years, despite being known about for over a century [1–3]. Solid particles that exhibit partial wettability with both of the fluid phases making up the emulsion are required; the particles reduce the free energy of the fluid–fluid interface and hence become kinetically trapped. It is therefore possible to create an emulsion stabilised solely by solid particles, where each droplet is coated with a layer of particles [4]. However, if the particles protrude further into the continuous phase than they do into the dispersed phase then it is possible for a particle to be adsorbed at two fluid–fluid interfaces simultaneously, a situation referred to as bridging [5,6] and shown schematically in Fig. 1(a and b).

Droplets which are bridged by particles may impart superior stability to the emulsion and hence be desirable in some cases [7]. However, bridging will often be undesirable, as creaming rates will be enhanced and the emulsion may flow poorly. The microstructure of bridged Pickering emulsions has previously been studied using confocal microscopy by Lee et al. [8] and Xu et al. have demonstrated that bridging can occur when particles on opposing interfaces interlock as they come together, but also that the bridging particles can initially all come from one interface [9]. Work has also recently been done on bridging in immiscible polymer blends. Moghimi et al. have shown that the presence of bridging particles significantly alters the rheology of their emulsions, and inhibits flow-induced coalescence [10]. Nagarkar and Velankar have also shown that particle bridges can occur in immiscible polymer blends and lend the blends a solid-like rheology [11]. Destribats et al. have investigated the bridging behaviour of emulsions stabilised by soft microgel particles and found that the emulsion's flocculation behaviour is highly dependent on the nature of the particle interactions during the emulsification process [12]. Particle bridging in Pickering systems where one of the fluid phases is an ionic liquid has been studied by Frost et al., who observed clusters of droplets held together by monolayers of particles [13,14].

Whether desirable or undesirable, it is important to understand the mechanisms involved in creating bridged emulsions, and how to choose system parameters to obtain the desired emulsion characteristics. We have therefore studied various methods of both

* Corresponding author.
E-mail address: David.French@ed.ac.uk (D.J. French).

http://dx.doi.org/10.1016/j.jcis.2014.11.032
0021-9797/© 2014 The Authors. Published by Elsevier Inc.
This is an open access article under the CC BY license (http://creativecommons.org/licenses/by/3.0/).

creating and breaking up droplet aggregates, and the ways these are affected by system parameters.

In the rest of this paper we will briefly describe some necessary quantitative considerations and our experimental methods, before describing our experimental results in two broad themes: firstly how particle bridges are formed, and then how particle bridges can be removed from an emulsion.

1.1. Quantitative considerations

The location of a particle at the oil–water interface is characterised by the three-phase contact angle, θ_w, which is measured through the more polar liquid phase, as shown in Fig. 1(c). The contact angle is described by the Young equation, relating the solid–oil, solid–water and oil–water interfacial tensions:

$$\sigma_{so} = \sigma_{sw} + \sigma_{ow}\cos\theta_w \tag{1}$$

where the subscripts s, o and w refer to the solid, oil and water phases respectively. The energy, G, required to remove a particle of radius r from the oil–water interface into its preferred phase is given by:

$$G = \pi r^2 \sigma_{ow}(1 - |\cos\theta_w|)^2 \tag{2}$$

which for micrometre-sized particles and a contact angle of 90° is typically $\gtrsim 10^6\, k_B T$, meaning particles are usually irreversibly adsorbed. It can be seen that the most strongly adsorbing particles are those which are wetted equally by both fluids, but even for smaller contact angles of, say, 30°, the attachment energy is still usually $\gtrsim 10^4\, k_B T$.

The volume fractions and sizes of the dispersed and solid phases are related by:

$$d_o = \frac{2\pi}{\sqrt{3}}\frac{\phi_o d_p}{\phi_p} \tag{3}$$

where d_o is the droplets' diameter, ϕ_o is the volume fraction of oil, d_p is the particles' diameter and ϕ_p is the volume fraction of particles.[1]

The degree of aggregation of droplets in an emulsion can be quantified using the fraction of water resolved, f_w, which is given by:

$$f_w = \frac{h_w}{h_t \phi_w} \tag{4}$$

where h_w is the height of the resolved water, h_t is the total height of the sample and ϕ_w is the volume fraction of water. Larger values of f_w mean that the emulsion droplets have packed more densely, a process which is hindered by droplet aggregation. For random close packing of monodisperse droplets in a sample with $\phi_o = 0.2$, the expected value is $f_w = 0.85$. Polydispersity will tend to increase packing efficiency (increase f_w). Meniscus effects are ignored here, but will not vary greatly between samples.

In order for particle bridging to occur, the particles must have a contact angle, θ_w, of less than 90°, otherwise the two droplets would overlap and coalesce. Bridging will also only occur between partially coated droplets, as fully coated droplets are mechanically stable to coalescence. Shearing of an already emulsified sample will create extra oil–water interface. Coalescence between partially-coated droplets can then reduce the amount of oil–water interface until the droplets are fully coated, or particles on one partially-coated droplet can adsorb to another, also reducing the amount of oil–water interface. Fig. 1(d) depicts the sensitivity of particle bridging to the contact angle.

[1] The numerical pre-factor has been corrected from Ref. [15].

1.2. Theory of emulsification

In laminar flow the capillary number, Ca, is used to explain the relationship between interfacial area and shear rate. It is defined as the ratio of viscous forces to interfacial forces:

$$Ca = \frac{\eta\dot{\gamma}R}{\sigma_{ow}} \tag{5}$$

where η is the viscosity of the continuous phase, $\dot{\gamma}$ is the shear rate and R is the radius of a droplet. If Ca is above a critical value, Ca_c, then a droplet will burst, reducing R and hence Ca [16]. At the same time, small droplets can coalesce, causing R and Ca to increase. In this way, Ca will tend towards Ca_c, the exact value of which depends on the viscosities of the dispersed and continuous phases, but is approximately 0.2 in the experiments carried out here. This allows us to re-express Eq. (5) as

$$A = \frac{3V_d}{Ca_c}\frac{\eta\dot{\gamma}}{\sigma_{ow}} \tag{6}$$

where A is the total interfacial area and V_d is the total volume of the dispersed phase.

Under turbulent conditions, however, droplet breakup is facilitated by stress from eddies and Eq. (5) is no longer valid. Instead, the maximum droplet size which will not break up, d_{max}, is given by:

$$d_{max} = C\frac{\sigma_{ow}^{3/5}}{\rho^{1/5}\epsilon^{2/5}} \tag{7}$$

where ρ is the density of the continuous phase, ϵ is the energy dissipated per unit volume and per unit time, and C is an unknown proportionality constant, thought to be approximately 1 [17]. This equation can also be re-expressed to give the interfacial area:

$$A = \frac{6V_d\rho^{1/5}\epsilon^{2/5}}{\sigma_{ow}^{3/5}} \tag{8}$$

We have used two different emulsification devices, a rotor–stator and a vortex mixer, to emulsify and shear our samples. The rotor–stator is capable of generating controlled shear rates over a large range, from 0 to 53 000 s^{-1}. The residence time of the rotor–stator can be estimated as

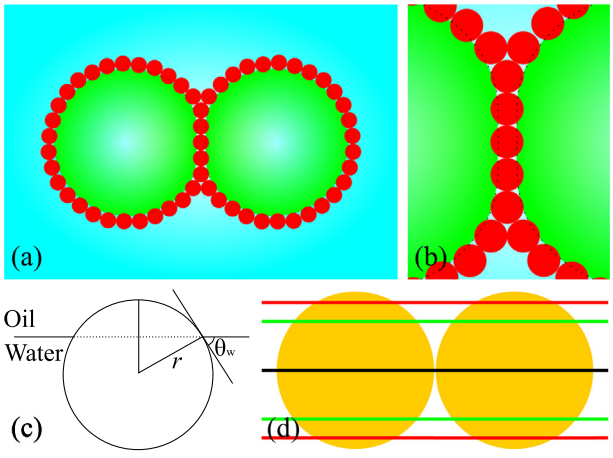

Fig. 1. (a) Cartoon showing two droplets bridged by particles. (b) Enlarged section, showing the layer of water between the two droplets. (c) Definition of the three-phase contact angle. (d) If the contact angle is close to, or above, 90° then bridging cannot occur (black line), whilst if it is too small then the particle attachment energy will be too low to maintain stability (red lines). Instead, an intermediate contact angle is required (green lines).

$$\tau_{res} \approx \frac{\delta}{r_{in}\omega} \tag{9}$$

where δ is the width of the gap between the rotor and the stator, r_{in} is the inner radius of the stator and ω is the angular velocity of the rotor, in rad s^{-1}. The vortex mixer has a much larger shear zone than the rotor–stator, meaning that the droplets it creates have a longer lifetime, which can make it easier to get all the particles in a sample onto an oil–water interface.

Sparks has estimated that $\approx 3\%$ of the power supplied to the rotor–stator is dissipated in the fluid through turbulence [18], and that this dissipation occurs in a relatively small volume surrounding the rotor and stator. Given the maximum power output and maximum shear rate, which are 750 W and 53 000 s^{-1} respectively, and assuming that the power dissipated is proportional to the square of the shear rate we can then estimate ϵ for our rotor–stator:

$$\epsilon = 0.03 \times 750\left(\frac{\dot{\gamma}}{53\,000}\right)^2\left(\frac{1}{(2 \times r_{in})^3}\right). \tag{10}$$

Whether the flow is laminar or turbulent can be determined from the Reynolds number, *Re*, given by:

$$Re = \frac{vl\rho}{\eta} \tag{11}$$

where v is a characteristic velocity, here the tip velocity of the rotor, and l is a characteristic length scale, here the width of the gap between the rotor and the stator. If $Re \gtrsim 1000$, the flow will be turbulent.

It is not yet clear, however, how the solid layer of particles at a droplet's interface affects the interface's mechanical properties and Ca_c. This is an active area of research; recent work by Maurice et al. [19] and by Hermes and Clegg [20] is beginning to address this problem.

In practice the viscosity of the continuous phase depends on the particle volume fraction, which is not constant during the emulsification process. We work, however, at particle volume fractions below 2.5%, and so the contribution to the viscosity from the colloidal particles is low.

2. Materials and methods

2.1. Sample preparation

Oil-in-water emulsions stabilised by fluorescent Stöber silica particles were prepared by mixing the oil phase with a dispersion of the particles.

Silica particles of radius 430 nm were prepared using a modified Stöber method to incorporate fluorescein isothiocyanate (FITC) dye [21]. The silica particles were washed ten times with distilled water to remove the ammonia, and then dried for one hour in a vacuum oven pre-heated to 170 °C, rendering the particles hydrophobic enough to sequester to the oil–water interface [22].

Dispersions of silica were prepared as follows. Dried silica was added to 2.33 ml of water (resistivity of at least 18 MΩ cm) and dispersed using a pulsed ultrasonic probe to avoid overheating. A typical dispersion protocol involved 1 s of sonication followed by 5 s of no sonication, repeated for a total time of 6 min. 0.67 ml of the oil phase, a mixture of dodecane (Sigma–Aldrich, $\geqslant 99\%$) and isopropyl myristate (Sigma–Aldrich, $\geqslant 98\%$), was then added prior to the initial emulsification, which was carried out by vortex mixing until the resolved water was clear, or until further mixing did not decrease the opacity of the resolved water. In most cases, this takes several minutes, but at lower particle volume fractions ($\lesssim 0.75\%$) can be done in 15 s. The volume fraction, Φ_{IM}, of isopropyl myristate in the oil phase is used to control particle wettability [23]. The oil volume fraction was 20%. Subsequent shearing of samples was carried out using a rotor–stator device (Kinematica polytron – inner diameter 5 mm, gap size 0.15 mm) at shear rates between 8000 s^{-1} and 34 000 s^{-1}. Particle volume fractions are calculated assuming a particle density of 1750 kg m^{-3} [21].

The droplet size predicted by Eq. (3) for these system parameters, and a particle volume fraction of 1.0%, is ≈60 μm.

In order to modify the inter-particle electrostatic interactions, sodium chloride (VWR, 99.9%) was added to some silica dispersions. Glycerol (Fisher, $\geqslant 98\%$) was added in order to modify the van der Waals interactions and the viscosity of the aqueous phase. Hydrochloric acid (Fluka, 1.0 M) and sodium hydroxide (Fisher, 98.73%) were added to samples to adjust their pH.

2.2. Electron microscopy

Samples for freeze-fracture scanning electron microscopy (FFSEM) were mounted in copper chalices which were used to fracture the samples. A copper collar was placed on a chalice and then the Pickering emulsion was added to the chalice using a pipette until the meniscus protruded above the collar. Liquid nitrogen was used to freeze the sample in a Gatan Alto 2500 cryotransfer system and the sample was then transferred to the preparation chamber which was at −124 °C and under high vacuum. Sample fracture was carried out by knocking the copper collar off the chalice with a cooled scalpel blade within the preparation chamber. The sample was then heated to −96 °C for two minutes to allow ice to sublime. Following sublimation, the sample was again cooled to −124 °C and sputter coated with ≈6 nm platinum. The sample was then transferred to a Gatan cold stage in a Hitachi S-4700 field emission scanning electron microscope, where it was maintained

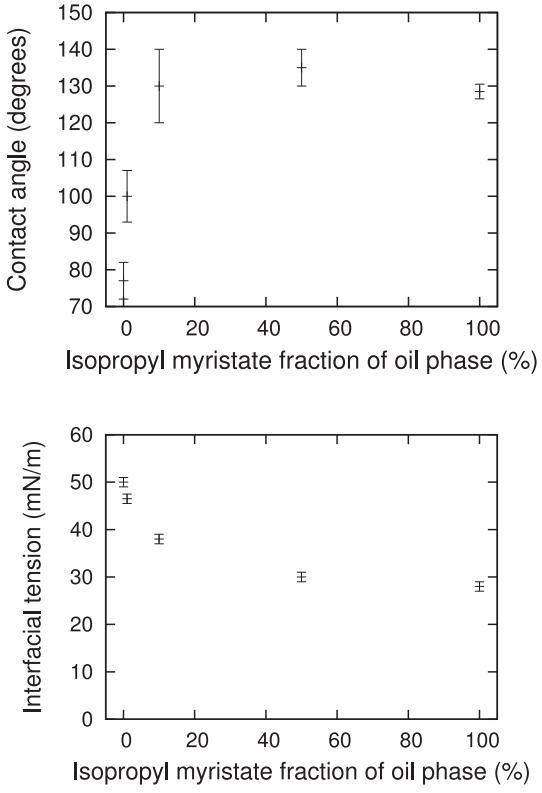

Fig. 2. Top: Dependence of θ_w on the isopropyl myristate fraction of the oil phase. Bottom: Dependence of the oil–water interfacial tension on the isopropyl myristate fraction of the oil phase.

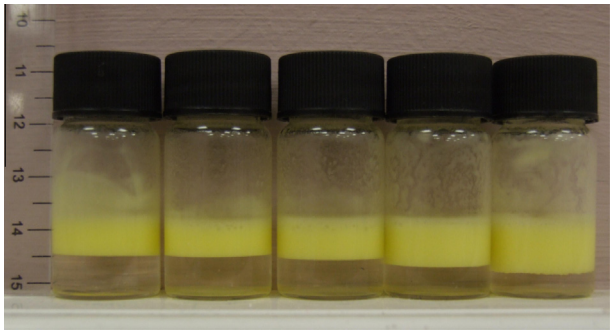

Fig. 3. Increasing shear rate (left to right) causes a decrease in emulsion packing fraction. The shear rates are, from left to right: vortex mixer only, 8500 s^{-1}, 17 000 s^{-1}, 25 500 s^{-1} and 34 000 s^{-1}. In all samples, $\phi_o = 20\%$, $\phi_p = 1.7\%$ and $\Phi_{IM} = 10\%$. The emulsion appears yellow due to the FITC dye in the silica particles, and the clear phase at the bottom is the resolved water.

at −124 °C and observed using an accelerating voltage of 5.0 kV at a working distance of 5 mm using both upper and lower secondary electron detectors.

2.3. Interfacial tension and contact angle measurements

Interfacial tension measurements were made using the pendant drop method with a Krüss EasyDrop tensiometer (model 65 FM40Mk2). The dodecane used for interfacial tension and contact angle measurements was filtered through alumina two times to remove polar impurities.

Contact angle measurements were performed using the sessile drop method with the same apparatus. Particles were dispersed in water, with $\phi_p = 30\%$, and spin-coated onto glass cover slips which were then left to dry overnight before use. Both advancing and receding contact angle measurements were made, and the average used as the equilibrium contact angle.

Fig. 2 shows how the three-phase contact angle and the oil–water interfacial tension depend on the oil phase's isopropyl myristate content. These results show that $\theta_w > 90^\circ$ for all but the 0% isopropyl myristate case, despite the silica particles forming stable dispersions in water but not in oil. This suggests that surface roughness of the spin-coated particle layer is affecting the contact angles. Nevertheless, the increase in θ_w as Φ_{IM} increases corroborates our belief that increasing the oil phase's isopropyl myristate content increases the wettability of the particles by the oil phase.

2.4. Light scattering

A Beckman Coulter LS 13 320 Particle Size Analyzer was used to measure the size distributions of emulsion droplets and aggregates of droplets.

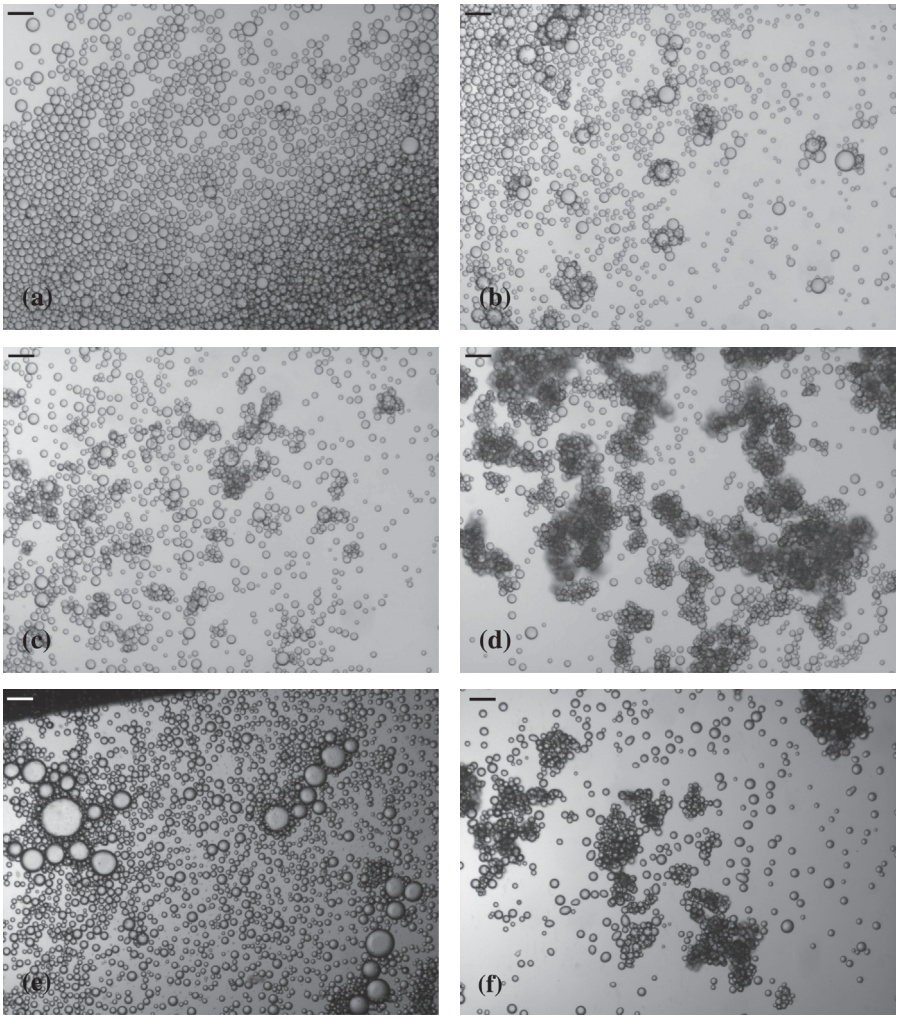

Fig. 4. (a–d) Micrographs of samples from Fig. 3 – (a) 8500 s^{-1}, (b) 17 000 s^{-1}, (c) 25 500 s^{-1}, (d) 34 000 s^{-1}. (e) The same sample as in (d), following further shear at 8500 s^{-1}. (f) The same sample as in (a), following further shear at 34 000 s^{-1}. Scalebars are 100 μm.

3. Results and discussion

We first describe the effects that shear rate, particle volume fraction and particle wettability have on droplet aggregation. These effects are explained in terms of the interfacial area generated during shear, with reference to Eqs. (5) and (7). We then discuss the effects of more complex shear histories on samples, and finally show that the addition of small quantities of sodium chloride or glycerol destabilises the bridged system.

3.1. Bridge formation

3.1.1. Shear rate

As shown in Fig. 3, a decrease in emulsion packing fraction is observed when the shear rate is increased, together with an increase in the roughness of the emulsion-resolved water interface. The non-aggregating emulsions formed at low shear rates are reasonably monodisperse (CV ≈ 25%) and have smooth emulsion-resolved water interfaces. The corresponding bright-field micrographs (Fig. 4) show that this is because the emulsions' propensity to aggregate increases with shear rate. The samples shown in Fig. 3 were prepared with $\phi_p = 1.7\%$ and $\Phi_{IM} = 10\%$ and then pre-emulsified using a vortex mixer, creating moderately aggregating emulsions with a primary droplet size of ≈30 μm, which is slightly lower than that predicted by Eq. (3) due to droplets sharing particles and a surface coverage which is lower than the theoretical maximum of close-packed spheres. A micrograph of a pre-emulsified sample is shown in Fig. 11. These samples were then subjected to a variety of shear rates using a rotor–stator device. Low shear rates ($\approx 8500\ s^{-1}$) create smooth, non-aggregating emulsions whilst progressively higher shear rates create increasingly flocculated networks of droplets, as shown in the micrographs in Fig. 4(a–d). This aggregating behaviour causes a decrease in the packing efficiency of the emulsion (Fig. 12). Even at the lowest shear rate f_w is only 0.65, notably lower than the value of 0.85 expected for random close packing – even without aggregation effects our samples do not pack closely.

As can be seen from Eqs. (5) and (7), increasing the shear rate will lower the droplet radius. This means that at higher shear rates, there will be a greater amount of interfacial area exposed, and so a greater number of collisions between partially coated droplets will take place. Since it is these collisions which lead to particle bridging, the degree of aggregation increases when shear rate is increased.

Using Eq. (11), we find that $Re \gtrsim 1000$ when $\dot{\gamma} \gtrsim 12\,500\ s^{-1}$. We have therefore used Eqs. (3), (7) and (10) to estimate the shear rate at which the interfacial area generated during shear will be greater than that which can be stabilised by the particles during this experiment. We find that the critical shear rate for these parameters is $\approx 21\,000\ s^{-1}$, which compares reasonably well with the observed onset of aggregation at $\approx 17\,000\ s^{-1}$.

3.1.2. Electron microscopy

FFSEM was used to look directly for particles bridging droplets. Samples were prepared with particle volume fractions of 0.6%, 1.1% and 1.7%, and $\Phi_{IM} = 10\%$. The electron micrographs, shown in Fig. 5, clearly show particles being shared by droplets and we find that this behaviour is more prevalent at lower particle volume fractions, an observation which will be explained below.

Analysis of the patterns left in the droplets where the particle layer has been ripped off during fracture show that $\theta_w \approx 30^\circ$. It is possible, however, that differences in freezing rates and expansivities between the two liquid phases will affect this.

3.1.3. Particle wettability

We find that increasing the volume fraction of isopropyl myristate in the oil phase makes particles more likely to adsorb to the interface. When $\phi_p \gtrsim 1.0\%$ and $\Phi_{IM} = 0\%$ it is impossible to sequester all the particles to an oil–water interface using only a vortex mixer, even after 5 min of mixing, but if $\Phi_{IM} \gtrsim 10\%$ the sample can be fully emulsified in less than a minute. This can be seen in Fig. 6, where it is only at higher isopropyl myristate volume

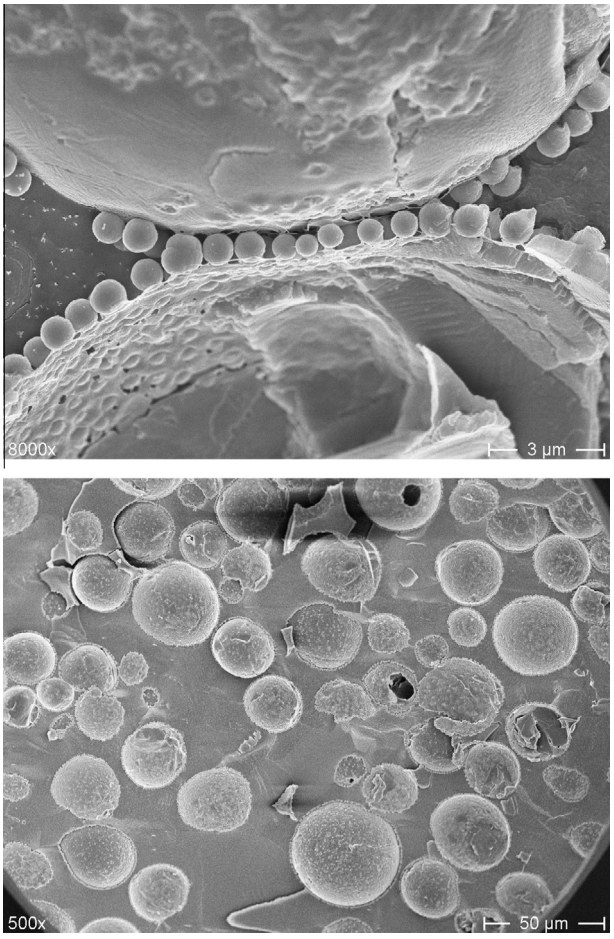

Fig. 5. Top: Freeze-fracture scanning electron microscope image of silica particles being shared by two droplets. This emulsion was prepared with ϕ_o = 20%, ϕ_p = 0.6%, $\Phi_{IM} = 10\%$ and was sheared at 34 000 s^{-1}. Bottom: FFSEM image of an emulsion prepared with ϕ_o = 20%, ϕ_p = 1.7% and $\Phi_{IM} = 10\%$, which was sheared at 34 000 s^{-1}, showing that most droplets are not aggregated.

Fig. 6. Increasing particle wettability by the dispersed phase (left to right) causes a decrease in emulsion packing fraction. Φ_{IM} values are 0%, 1%, 10%, 50% and 100%. ϕ_o and ϕ_p are 20% and 1.7% respectively. The samples were sheared at 17 000 s^{-1} for 8 min.

fractions that the resolved water becomes fully depleted of particles. We attribute this to the lower interfacial tension of isopropyl myristate with water, relative to that of dodecane with water (Fig. 2), as well as its higher dielectric constant. These changes mean that a particular shear rate will generate more interfacial area when isopropyl myristate is included, since the interfacial area is inversely proportional to σ_{ow} when the flow is laminar (Eq. (6)), and proportional to $\sigma_{ow}^{-3/5}$ when the flow is turbulent (Eq. (8)). Additionally, there will be an increased particle-interface attraction. We also find that increasing Φ_{IM} increases an emulsion's degree of aggregation, as shown in Fig. 6.

The propensity of an emulsion to aggregate via particle bridging will be affected by the three-phase contact angle. If the particles are neutrally wetting ($\theta_w = 90^\circ$) or preferentially wetted by the dispersed phase then it will be impossible for a particle to be shared between two droplets. On the other hand, if the contact angle is too small, then the attachment energy of the particle decreases and the emulsion becomes unstable. At intermediate contact angles, $\theta_w \approx 30$—70°, particle bridging should be possible. Increasing Φ_{IM} increases the contact angle of the particles at the interface, and this will affect particle bridging.

Variations in Φ_{IM} therefore affect both the contact angle and the interfacial tension, as well as the particle-interface interactions. Whilst all of these effects, and others, will contribute to the observed changes in particle bridging when Φ_{IM} is varied, we believe that the most important aspect is the lowering of the interfacial tension, as this leads to a large increase in the number of droplets in the emulsion during the shearing process, and hence increases the number of collisions between partially coated droplets. The other changes, such as contact angle, will be secondary effects to this.

3.1.4. Droplet size distribution

The aggregating nature of the emulsions can also be demonstrated using the apparent droplet size as measured using light scattering. Fig. 7 shows that the apparent droplet size increases as shear rate is increased. This is because the light scattering apparatus is measuring the size of clusters of aggregated droplets, rather than the primary droplet sizes. It is also interesting to note that the primary droplet size, which can be approximated by the left hand peak on each graph, is roughly unchanged, *i.e.* aggregation occurs without significant changes in the primary droplet size, which is determined by the particle volume fraction.

3.1.5. Particle volume fraction

We find that increasing the particle volume fraction decreases an emulsion's propensity to aggregate, for a given shear rate, as shown in Fig. 8. The emulsion-resolved water interfaces in the

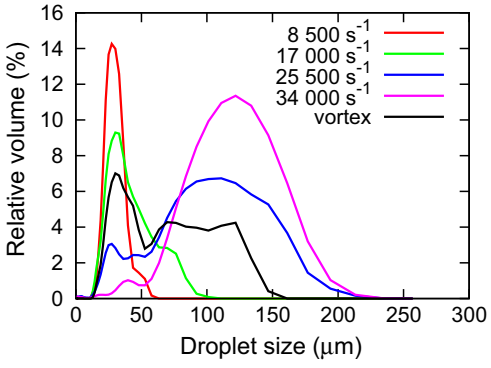

Fig. 7. Apparent droplet sizes, measured using light scattering. The emulsions were prepared with $\phi_o = 20\%$, $\phi_p = 1.7\%$ and $\Phi_{IM} = 10\%$.

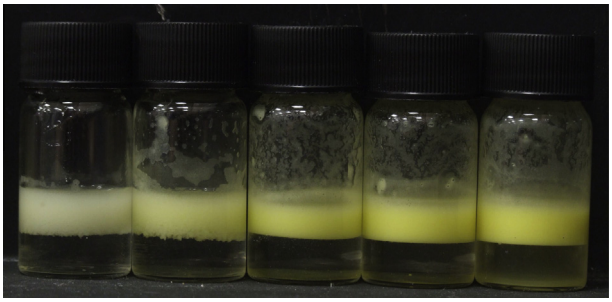

Fig. 8. Increasing particle volume fraction (left to right) leads to the formation of emulsions which are more densely packed. Particle volume fractions are, from left to right, 0.3%, 0.6%, 1.1%, 1.7% and 2.3%. In all samples, $\phi_o = 20\%$ and $\Phi_{IM} = 10\%$. All samples were sheared at 17 000 s^{-1} for 8 min.

samples with lower particle volume fractions are rough because these samples contain clusters of aggregated droplets, caused by particle bridging. The smoother emulsion-resolved water interfaces in the samples with higher particle volume fractions show that these samples contain significantly fewer particle bridges. The interfacial area during shear is determined by Eq. (6) or (8), and the proportion of this area which is covered by particles is determined by ϕ_p. If the interfacial area exceeds that which can be occupied by particles, then particle bridging can occur.

When using an oil phase with $\Phi_{IM} = 10\%$ and a particle volume fraction below 1.25%, it is observed that the entire emulsion creams rapidly, suggesting that the vast majority of droplets have formed aggregates. When ϕ_p is 1.25% or greater, however, a single emulsion is observed to have two populations of droplets creaming at different rates: there is a rapidly creaming portion comprised of aggregated droplets and a slowly creaming portion, comprised of non-aggregated droplets. This suggests that the population of slowly creaming droplets are those which quickly become fully coated with particles.

The presence of free silica in a sample will also inhibit particle bridging. This can be seen when a sample with $\phi_p \approx 1.1\%$ is emulsified with a vortex mixer. Following initial mixing for 30 s a smooth emulsion is formed, but not all particles adsorb to a droplet interface. Further bursts of emulsification create increasingly aggregated emulsions with increasingly clear resolved water phases. This shows that free silica can prevent droplet aggregation from occurring, because the free silica will adsorb to the bare interface before another partially coated droplet can do so (Fig. 13).

Particle bridging relies on collisions occurring between partially coated droplets, and so bridging will only occur below a critical particle volume fraction, which will depend on the shear rate. Above this critical particle volume fraction, the applied shear will not create enough bare interface for a significant number of collisions to occur between partially coated droplets, as all collisions will be taking place between fully coated droplets. Using Eqs. (3), (7) and (10), we find that the critical particle volume fraction in this case is $\approx 1.4\%$, which compares relatively well with the observed onset of aggregation at $\approx 1.1\%$.

These results can be viewed in the context of the wider Pickering emulsion literature. As outlined in the introduction, a handful of researchers have studied bridging in Pickering emulsions. We suggest that there are other published results where bridging is likely to play a crucial role but where it has not been identified. Furthermore, the sample preparation route is not always sufficiently described to draw any clear conclusion. A case where the preparation protocol is described is Fig. 4 in Ref. [24]. Here, emulsions of PDMS-in-water were prepared under two different shear protocols: one protocol causes dispersed droplets to form whilst the other causes the droplets to form large aggregates which cream

rapidly. We conclude that the sample presented in Fig. 4(b) of Ref. [24] is dominated by particle bridging between droplets. A case where the preparation protocol is not sufficiently described is Fig. 6 of Ref. [25], where the rotation rate used to prepare the emulsion is either 13 500 rpm or 24 000 rpm. In Fig. 6(a and b) the samples containing the lowest concentration of particles result in the smallest, most strongly aggregating droplets, which could be a signature of particle bridging. In Ref. [25] all emulsion characteristics were attributed to particle wettability, ignoring the potential importance of the processing route.

Other examples of potentially bridged emulsions which have not been identified as such are Fig. 4 (71% SiOH sample) in Ref. [26], Fig. 3 in Ref. [27], Fig. 16 (0.05–0.2 M TEAB samples) in Ref. [28] and Fig. 10, in Ref. [29]. Additionally, in Ref. [30], the presence of bridging is identified in Fig. 12(g–i), but the flocculation observed in Fig. 12(b) and the decrease in the fraction of resolved water shown in Fig. 13(a and b) are not attributed to bridging.

3.2. Bridge breaking

Having described the processes by which particle bridges form in our system, we will now describe some of the processes which can lead to their removal.

3.2.1. Complex shear histories

We have investigated the effects of more complex shear histories on our emulsions. For example, if an emulsion is subjected to a high shear rate followed by a low shear rate we find that a bidisperse emulsion is produced, with a small number of larger droplets present, which have a diameter approximately three times that of the main population, as shown in Fig. 4(e). We believe this is caused by the coalescence of droplets which had previously been bridged together. Because some particles in the aggregates are shared by droplets, it is possible for coalescence to occur without any particles being removed from the water–oil interface. An aggregated emulsion can therefore de-aggregate without any silica appearing in the resolved water.

Fig. 10. Photograph of bridged emulsions taken immediately following pH adjustment. Sample pHs are, from left to right, 2, 4, 6, 7, 8 and 10. In all samples ϕ_o, ϕ_p and Φ_{IM} are 20%, 0.6% and 10% respectively. Emulsification was performed with a vortex mixer. The sample with an aqueous phase pH of 2 has undergone coalescence so that the droplets are ≈ 300 μm in diameter.

The fact that when an aggregated sample is sheared at a relatively low shear rate, the emulsion eventually becomes non-aggregated suggests that these low shear rates are capable of pulling two bridged droplets apart, and that coalescence events dominate over bridging events at lower shear rates. This could be a result of repulsive interactions between particles, which at lower droplet collision energies have enough time to create large bare patches on droplets, but at higher collision energies leave only smaller bare patches more prone to bridging events.

On the other hand, when a sample is sheared first at a relatively low shear rate and then at a relatively high shear rate, enough oil–water interface is created to make particle bridging likely. The sample in this case is also observed to contain non-spherical droplets, as shown in Fig. 4(f), which are not observed when the sample undergoes only the higher shear rate. It is not yet clear, however, if these effects are influenced by emulsion aging.

We have also studied the stability of the aggregated emulsions to very low shear rates by using roller banks. When the particle volume fraction is below ≈0.5%, the droplets are large enough that their buoyancy prevents them mixing well when on the roller bank, and the emulsion can remain unchanged even after several weeks. At higher particle volume fractions, the buoyancy of the droplets is lower and the roller bank is capable of a more thorough

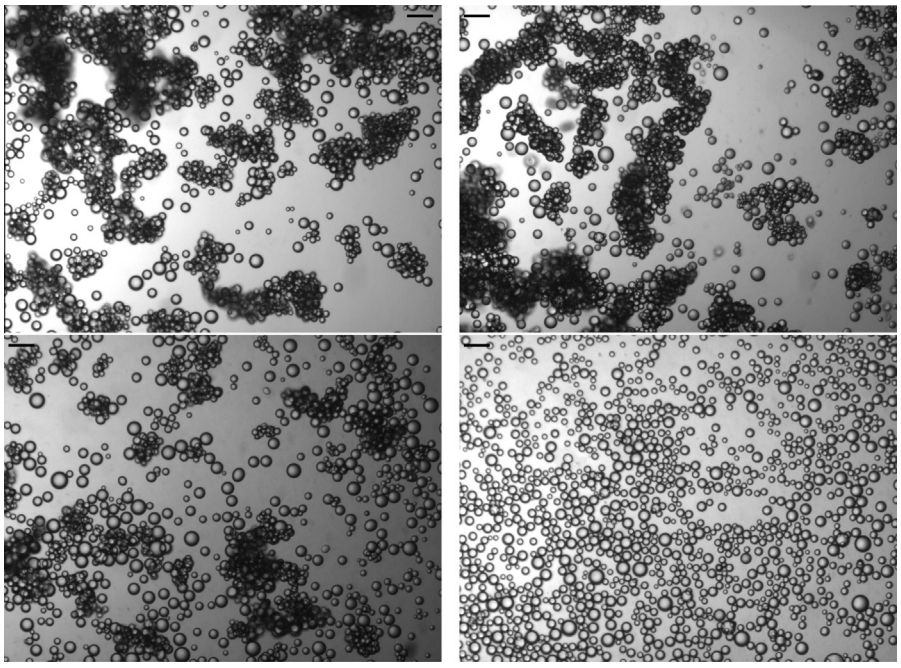

Fig. 9. The addition of salt to samples after emulsification destroys particle bridging. The salt concentrations are: Top: 0 mM and 5 mM, Bottom: 10 mM and 40 mM. The sample was created with ϕ_o = 20%, ϕ_p = 1.1%, Φ_{IM} = 10%, and sodium chloride was added in ≈5 mM increments, with the sample being shaken gently after each addition to dissolve the salt. Scalebars are 100 μm.

mixing. Under these circumstances, the emulsion de-aggregates but remains stable.

3.2.2. Changing wettability

3.2.2.1. Sodium chloride. The addition of small concentrations ($\lesssim 40$ mM) of sodium chloride to the silica dispersions prior to emulsification disrupts the system enough to prevent droplet aggregation occurring. Adding similarly small quantities of NaCl to aggregated emulsions, combined with gentle shaking to dissolve the salt, also disrupts the droplet network, creating a non-aggregated emulsion, as shown in Fig. 9. When the emulsion de-aggregates, free silica is observed in the resolved water. The addition of salt to the system causes θ_w to decrease, leading to a lower particle trapping energy [31]. This means that the droplet aggregates are less strongly held together, and so gentle shaking is enough to pull the aggregates apart. When this happens, bridged particles are removed from one, or occasionally both, of the two interfaces to which they had previously been attached, leading to a non-aggregated emulsion with a small amount of free silica in the resolved water.

Adding salt causes electrostatic interactions to be screened, which makes coalescence events between droplets more likely, since there are electrostatic repulsions between the particles on two droplets, and the oil droplets themselves have a slight charge on their surface. The Debye length, κ^{-1}, of an aqueous solution of a monovalent salt at room temperature is given by

$$\kappa^{-1} = 0.304 I^{-\frac{1}{2}} \text{ nm}. \quad (12)$$

where I is the salt concentration in moles per litre [32]. When two partially coated droplets come together, the reduced Debye length may have some influence on the likelihood of coalescence.

Two samples were created with different values of $\Phi_{IM} - 1\%$ and 50%, so that their interfacial tensions differed. In both samples $\phi_p = 1.1\%$ and $\phi_o = 20\%$. The two samples were emulsified initially using a vortex mixer, then sheared at 17 000 s^{-1} for 10 min and then again at 34 000 s^{-1} for two minutes, creating strongly aggregated emulsions. Sodium chloride was then gradually added to both emulsions, generally in 5 mM steps, and the emulsions were shaken gently to dissolve the salt. The sample with $\Phi_{IM} = 1\%$ was observed to de-aggregate at a salt concentration of approximately 15 mM, whilst the sample with $\Phi_{IM} = 50\%$ did not de-aggregate until the salt concentration was approximately 50 mM. If the main mechanism involved in de-aggregating the emulsions was the overcoming of an electrostatic repulsion between bridged droplets, then one would expect the sample with the lower interfacial tension (and hence weaker particle trapping) to de-aggregate at a lower salt concentration than the sample with the higher interfacial tension. Instead, it seems likely that the mechanism causing de-aggregation is a decrease in θ_w when the salt is added, which leads to a decrease in the attachment energy of the particles and means that the bridged droplets can be pulled apart by gently shaking the sample. However, because the oil phase changes in each case, it is not clear that the amount of charge on a droplet would be constant, but the gradual nature of the de-aggregation also suggests that the mechanism involves changes in contact angle. Furthermore, the separation between bridged droplets when $\theta_w = 70^\circ$, is approximately 300 nm, many times larger than the Debye length for all but the pure water case.

We have measured the contact angle, θ_w, of a water droplet on a slide which has been spin-coated with silica particles, surrounded by an oil phase with $\Phi_{IM} = 10\%$ for both the case where the water contains no salt and the case where the water contains 40 mM of sodium chloride. We find that if the slides are dried under vacuum for one hour at 50 °C, then θ_w in the pure water case is 104(4)° but in the 40 mM NaCl case is 71(1)° (Fig. 14).

3.2.2.2. Glycerol. Adding glycerol to the samples increases both the viscosity and the refractive index of the continuous phase. The increase in the refractive index means that the strength of van der Waals interactions between particles is reduced.

Glycerol was gradually added to strongly aggregated emulsions – so that the aqueous phase was up to 40% glycerol, by volume – and the samples gently shaken to mix the glycerol into the water. This caused the emulsion to become less aggregated, with a smooth emulsion-resolved water interface forming (Fig. 15). If water is added to the emulsion instead of glycerol, deaggregation still occurs, but more addition/shaking cycles are required. We believe this is because the increase in viscosity, and the associated increase in shear rate during shaking, in the glycerated sample makes disruption of particle bridges more likely. Similar behaviour is observed when the glycerol is added to the aqueous phase prior to emulsification (Fig. 16), suggesting that dilution of the emulsion is not responsible.

This is consistent with the claim that low shear causes deaggregation, but changes in the strength of particle–particle interactions may also play a role, as may changes to θ_w.

3.2.2.3. pH. To demonstrate that pH can also be used to destabilise the aggregated systems, we made a series of aggregated emulsions, all with an aqueous phase pH of 7, and then adjusted the pH of the samples by adding hydrochloric acid or sodium hydroxide, followed by gentle shaking of the samples. Fig. 10 shows that the aggregated emulsions are stable between pH 4 and 10, but become unstable at pH 2. When these samples are placed on a roller bank for 12 h, the samples with a pH below 5 phase separate completely, with the silica in the aqueous phase. This suggests that even at low pH $\theta_w < 90^\circ$, and that the high charge on the particles at low pH causes them to repel each other strongly enough to destabilise the emulsion. In contrast, the samples with a pH above 5 deaggregate but remain stable.

4. Conclusions

We have developed a model Pickering emulsion which allows us to investigate the effects of several parameters on the degree of particle bridging between droplets. In particular, we have found that bridging will only occur if the particles have a preference for the continuous phase, but that the strength of a bridge decreases as the particles move further into the continuous phase. This effect can be used to remove particle bridges from an emulsion without destabilising the droplets. Particle bridges can also be removed by applying low shear. We have used freeze-fracture SEM to directly observe particle bridging, something which has not been published before, to our knowledge.

Our results show that the most important prerequisites for forming particle bridges are that the particles have a preference for the continuous phase and that more interfacial area is generated during the mixing process than can be stabilised by the particles present. We are able to quantitatively describe some of the processes involved in forming bridges. From our work we suggest that bridging may be more prevalent in the Pickering emulsion literature than previously realised, and may have been missed in cases in which the emulsification protocol was not carefully considered (or, in one or two cases, even described). We suggest that Fig. 4(b) in Ref. [24], Fig. 6(a and b) in Ref. [25], Fig. 4 (71% SiOH sample) in Ref. [26], Fig. 3 in Ref. [27], Fig. 16 (0.05–0.2 M TEAB samples) in Ref. [28], Fig. 10 in Ref. [29] and Fig. 12(b) in Ref. [30] potentially show bridged samples. We strongly argue that the characteristics of Pickering emulsions depend on the shear history of the sample and that this must be documented.

We have also investigated several methods for removing particle bridges from emulsions. We have found that shearing a bridged emulsion at a shear rate lower than that necessary to create particle bridges will remove bridges. Modifying the particle wettability, *e.g.* by adding salt to the aqueous phase, can greatly reduce the shear rate and time needed for this to occur.

An understanding of these two processes – making and breaking particle bridges – allows for control over the degree of aggregation in a Pickering emulsion. This allows a practitioner to control the emulsion's packing fraction, and hence control an emulsion's macroscopic properties, *e.g.* the viscosity of an emulsion could be varied independently of dispersed phase volume fraction. Our results should therefore be relevant to anyone wishing to design a well controlled Pickering emulsion system.

Acknowledgments

We thank J. Foundling and C. Stain for their help with the electron microscopy, A.B. Schofield for synthesising the particles, the EPSRC and Syngenta for a CASE award to D.J.F., and Grant EP/J007404/1.

Appendix A. Supplementary material

Supplementary data associated with this article can be found, in the online version, at http://dx.doi.org/10.1016/j.jcis.2014.11.032.

References

[1] B.P. Binks, T.S. Horozov, Colloidal Particles at Liquid Interfaces, Cambridge University Press, Cambridge, 2006.
[2] S.U. Pickering, J. Chem. Soc. 91 (1907) 2001–2021.
[3] W. Ramsden, Proc. R. Soc. London 72 (1903) 156–164.
[4] R. Aveyard, B.P. Binks, J.H. Clint, Adv. Colloid Interface Sci. 100 (102) (2003) 503–546.
[5] E.J. Stancik, M. Kouhkan, G.G. Fuller, Langmuir 20 (2004) 90–94.
[6] T.S. Horozov, B.P. Binks, Angew. Chem. Int. Ed. 45 (2006) 773–776.
[7] E.J. Stancik, M. Kouhkan, G.G. Fuller, Langmuir 20 (2004) 4805–4808.
[8] M.N. Lee, H.K. Chan, A. Mohraz, Langmuir 28 (2012) 3085–3091.
[9] H. Xu, M. Lask, J. Kirkwood, G. Fuller, Langmuir 23 (2007) 4837–4841.
[10] E. Moghimi, F. Goharpey, R. Foudazi, Rheol. Acta 53 (2014) 165–180.
[11] S.P. Nagarkar, S.S. Velankar, Soft Matter 8 (2012) 8464–8477.
[12] M. Destribats, V. Lapeyre, E. Sellier, F. Leal-Calderon, V. Ravaine, V. Schmitt, Langmuir 28 (2012) 3744–3755.
[13] E.M. Walker, D.S. Frost, L.L. Dai, J. Colloid Interface Sci. 363 (2011) 307–313.
[14] D.S. Frost, J.J. Schoepf, E.M. Nofen, L.L. Dai, J. Colloid Interface Sci. 383 (2012) 103–109.
[15] B.P. Binks, S.O. Lumsdon, Langmuir 17 (2001) 4540–4547.
[16] R.G. Larson, The Structure and Rheology of Complex Fluids, Oxford University Press, New York, 1999.
[17] P. Walstra, P.E.A. Smulders, in: B.P. Binks (Ed.), Modern Aspects of Emulsion Science, Royal Society of Chemistry, Cambridge, 1998 (Chapter 2).
[18] T. Sparks, Fluid Mixing in Rotor/Stator Mixers, PhD thesis, Cranfield University, 1996.
[19] L. Maurice, R.A. Maguire, A.B. Schofield, M.E. Cates, P.S. Clegg, J.H.J. Thijssen, Soft Matter 9 (2013) 7757–7765.
[20] M. Hermes, P.S. Clegg, Soft Matter 9 (2013) 7568–7575.
[21] A. van Blaaderen, A. Vrij, Langmuir 8 (1922) 2921–2931.
[22] K.A. White, A.B. Schofield, P. Wormald, J.W. Tavacoli, B.P. Binks, P.S. Clegg, J. Colloid Interface Sci. 359 (2011) 126–135.
[23] W.J. Frith, R. Pichot, M. Kirkland, B. Wolf, Ind. Eng. Chem. Res. 47 (2008) 6434–6444.
[24] S. Arditty, V. Schmitt, F. Lequeux, F. Leal-Calderon, Eur. Phys. J. B 44 (2005) 381–393.
[25] B.P. Binks, S.O. Lumsdon, Langmuir 16 (2000) 3748–3756.
[26] B.P. Binks, P.D.I. Fletcher, B.L. Holt, P. Beaussoubre, K. Wong, Phys. Chem. Chem. Phys. 12 (2010) 11954–11966.
[27] S. Arditty, V. Schmitt, J. Giermanska-Kahn, F. Leal-Calderon, J. Colloid Interface Sci. 275 (2004) 659–664.
[28] B.P. Binks, S.O. Lumsdon, Phys. Chem. Chem. Phys. 1 (1999) 3007–3016.
[29] B.P. Binks, S.O. Lumsdon, Langmuir 16 (2000) 8622–8631.
[30] B.P. Binks, R. Murakami, S.P. Armes, S. Fujii, Langmuir 22 (2006) 2050–2057.
[31] L.G.J. Fokkink, J. Ralston, Colloid. Surface. 36 (1989) 69–76.
[32] J.N. Israelachvili, Intermolecular and Surface Forces, Academic Press, London, 1992.